INTERNATIONAL JOURNAL FOR INNOVATIVE RESEARCH IN MULTIDISCIPLINARY FIELD
ISSN(O): 2455-0620 [Impact Factor: 9.47]
Monthly, Peer-Reviewed, Refereed, Indexed Journal with IC Value : 86.87
Volume - 11, Issue - 08, August - 2025

DOIs:10.2015/IJIRMF/202508008 --:-- Research Paper / Article / Review

Bayesian Optimization for Machine Learning–Based Diagnosis of Soft Faults in DC–DC Converters Using ICEEMDAN

[1] Mabia Khatun, [1] Md. Ariful Islam, [2] Merina Akter
[1]Masters of Electrical Engineering, Anhui University of Science and Technology, Huainan, Anhui, China
[1]Masters of Mechanical Engineering, Changan University, xian, China
[2]Masters of Computer Science and Technology, Changan University, xian, China

Email - [1]mabiakhatun.njpichina@gmail.com, [1]arifkhan271848@gmail.com, [2]merinahawla1999@gmail.com

Abstract: *Soft faults in DC–DC converters gradually degrade* their performance; however, *conventional threshold-based methods often fail to detect these subtle issues. This study proposes a framework that leverages advanced signal processing and machine learning to diagnose* soft-faults*. The converter voltage signal is decomposed using Improved Complete Ensemble Empirical Mode Decomposition with Adaptive Noise (ICEEMDAN) into intrinsic mode functions (IMFs). These IMFs* were *then denoised* using *wavelet thresholding to remove high-frequency noise. Time-domain statistical features (mean, root-mean-square, skewness,* and kurtosis*) are extracted from the denoised IMFs. The resulting feature vectors* were *used to train three classifiers: Support Vector Machine (SVM), Extreme Learning Machine (ELM), and XGBoost.* The hyperparameters of each *classifier* were optimised *using Bayesian* optimisation*. The ICEEMDAN-based features* achieved a *classification accuracy* of 95.6 *%(without tuning),* which was *significantly higher than the 88.9% accuracy* achieved with the *basic EMD. With Bayesian-tuned XGBoost,* the *accuracy* further improves*. The proposed integrated framework (ICEEMDAN decomposition → denoising → feature extraction →* Bayesian-optimised *classification) effectively exposes soft faults by mitigating* the *noise and mode mixing. This enhanced fault detection is valuable for critical applications* in which *undetected defects can lead to costly failures.*

Key Words: *Bayesian optimization; DC–DC converter; fault detection; ICEEMDAN; machine learning; soft faults; wavelet denoising.*

1. INTRODUCTION

DC–DC converters play a vital role in many industries (e.g. aerospace, power grids, and renewable energy) owing to their ability to efficiently regulate voltage levels (1); (2). However, converters are susceptible to both hard faults (e.g. short/open circuits) and soft faults (e.g. component aging and parameter drift). Soft faults manifest as minor performance degradations, such as slight overshoots or waveform distortions, which may be overlooked by conventional monitors (3). Although they do not cause immediate failure, soft faults gradually undermine reliability, making early detection essential to prevent costly downtimes and repairs.

Conventional threshold-based monitoring methods often struggle with soft faults because the deviations they cause remain within the normal operating range and can be masked by the routine variability. To address this challenge, machine learning techniques have gained interest for their ability to detect subtle patterns in sensor data that may indicate soft faults (4). Prior studies have employed signal decomposition methods (such as Empirical Mode Decomposition (EMD) and wavelet transforms) in combination with classifiers such as Support Vector Machines (SVM) and neural networks (5). For example, Huang et al. introduced EMD (6), which has been widely used in non-linear, non-stationary signal analysis, and Torres et al. proposed CEEMDAN (7) to mitigate EMD's limitations. Donoho (8) and Yan & Gao (9) demonstrated the benefits of wavelet thresholding in denoising high-frequency signal components while retaining the fault-sensitive characteristics. In parallel, machine learning models such as SVMs (10), ELMs (11), and

gradient-boosted trees (12) have gained popularity for fault classification owing to their generalisation capabilities. However, fixed hyperparameters in these models often lead to suboptimal performance. Bayesian optimisation provides a probabilistic and sample-efficient method for tuning hyperparameters and has recently gained traction in industrial diagnostic systems.

Despite these advances, limited studies have fully integrated adaptive decomposition (ICEEMDAN), wavelet-based denoising, and Bayesian-optimised classification. This study addresses this gap by proposing a unified diagnostic pipeline for soft-fault identification in DC–DC converters. Our contributions are:

Despite these advances, limited studies have fully integrated adaptive decomposition (ICEEMDAN), wavelet-based denoising, and Bayesian-optimised classification. This study addresses this gap by proposing a unified diagnostic pipeline for soft-fault identification in DC–DC converters. Our contributions are:

- We developed an integrated framework combining ICEEMDAN decomposition, wavelet denoising, and statistical feature extraction to analyse DC–DC converter signals.
- We applied and compared three machine learning models (SVM, ELM, and XGBoost) for multiclass soft-fault classification using the extracted features.
- We enhanced the classification performance by implementing Bayesian optimisation for automated hyperparameter tuning.
- We validated the proposed method using experimental data and compared its performance with those of the conventional EMD and CEEMDAN-based approaches under clean and noisy conditions.

2. LITERATURE REVIEW

Several studies have explored fault detection in power electronic systems, particularly DC–DC converters, using both traditional signal processing and modern machine learning techniques (4). Huang et al. introduced Empirical Mode Decomposition (EMD), which has since been widely applied in nonlinear, non-stationary signal analysis (13). However, the EMD suffers from mode mixing, which reduces its effectiveness in practical diagnostics. Torres et al. (7) proposed CEEMDAN, which mitigates some of these limitations by adding adaptive noise during the decomposition. Colominas et al. (14) further improved this with ICEEMDAN, enhancing decomposition reliability.

Donoho (8) and Yan & Gao (9) demonstrated the effectiveness of wavelet thresholding in denoising high-frequency signal components while retaining the fault-relevant characteristics. In parallel, machine learning methods such as support vector machines (SVMs) (10), extreme learning machines (ELMs) (11), and gradient-boosted trees (12) have gained popularity for fault classification owing to their generalisation capabilities and efficiency. However, fixed hyperparameters in such models often lead to suboptimal performance. Bayesian optimisation provides a probabilistic method for tuning these hyperparameters and has recently been applied in industrial diagnosis scenarios.

Despite these advances, the literature shows that limited work has fully combined adaptive signal decomposition (ICEEMDAN), wavelet-based denoising, and Bayesian-optimised classification. We propose to fill this gap by integrating these techniques into a unified diagnostic pipeline for soft faults in DC–DC converters.

3. OBJECTIVES

The primary objectives of this study are as follows:

1. To develop an integrated framework combining ICEEMDAN decomposition, wavelet denoising, and statistical feature extraction for analysing DC–DC converter signals.
2. To apply and compare three machine learning models (SVM, ELM, and XGBoost) for soft-fault classification using extracted features.
3. We enhanced the classification performance by implementing Bayesian optimisation for automated hyperparameter tuning.
4. The proposed method was validated using experimental data, and its performance was compared with that of the conventional EMD and CEEMDAN-based approaches under clean and noisy conditions.

4. METHODOLOGY

4.1 Feature Extraction Process

Feature extraction is crucial for transforming raw time-series data into representations that can be analysed using machine learning algorithms. We propose a three-stage feature extraction framework: ICEEMDAN decomposition, wavelet denoising, and statistical feature computation. This process captures the key signal characteristics required to distinguish between faulty and healthy conditions. First, the complex voltage signal is decomposed into simpler oscillatory components, called intrinsic mode functions (IMFs). Second, the noise in each component was reduced via wavelet denoising. Third, statistical features are extracted from the denoised components. Figure 1 illustrates the overall feature extraction process.

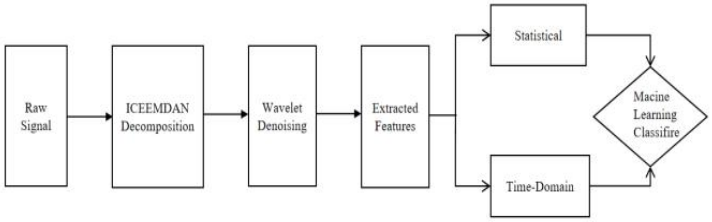

Figure.1. Proposed Feature Extraction Method

ICEEMDAN Decomposition

In the first stage, ICEEMDAN was applied to the raw signal. ICEEMDAN (14) extends the traditional Empirical Mode Decomposition (13) by adding adaptive white noise during the sifting process, which significantly reduces mode mixing. Through the iterative addition of noise and calculation of local means, ICEEMDAN extracts a series of distinct IMFs from the signal. Formally, the signal is decomposed as follows:

$$x(t)=\sum_{i=1}^{N}\mathrm{IMF}_i(t)+r_N(t)$$

where is the th intrinsic mode function, and is the final residual trend. In practice, the signal typically yields approximately 4–6 IMFs, with the residual becoming a monotonic baseline. Compared with classic EMD (6), ICEEMDAN ensures that each IMF is physically meaningful and contains significantly less spurious noise. This makes ICEEMDAN particularly suitable for detecting subtle degradation patterns from soft faults in DC–DC converters.

Wavelet Denoising

After decomposition, each IMF may still contain a high-frequency noise. We applied a discrete wavelet transform (DWT) to each IMF and performed soft thresholding (8) to suppress noise. Specifically, the high-frequency detail coefficients were thresholded to remove noise while preserving important signal features. The denoised IMFs were then reconstructed. This denoising step enhances the clarity of the modes and helps isolate the fault-induced variations. Finally, these denoised IMFs are summarised by time-domain statistics: for each IMF, we compute the mean, root mean square (RMS), variance, skewness, and kurtosis. These statistics quantify the amplitude distributions and waveform characteristics that reflect component degradation. Concatenating all selected IMF features yields a feature vector that is sensitive to the subtle changes caused by soft faults.

Time-Domain Feature Extraction

We extracted statistical features that are discriminative of faults from each denoised IMF. Our implementation computes metrics such as the maximum, minimum, peak-to-peak, mean, root mean square (RMS), variance, standard deviation, skewness, kurtosis, waveform factor, peak factor, pulse factor, mean square value, and clearance factor. These 14 features capture both the dimensional (e.g. peak values and RMS) and dimensionless (e.g. skewness and kurtosis) properties of the signal, improving noise robustness. Table 1 summarises these time-domain features and their

corresponding calculations. The combined set of features from all the IMFs forms the input for the classifiers. This rich feature set enables the detection of subtle variations in the system behaviour, which often signal soft faults.

Table 1. Time-Domain Features Extracted from Each Denoised IMF.

Feature (Symbol)	Formula	Feature (Symbol)	Formula
Max value X_{max}	$\max(x_i)$	*Skewness* -	$\frac{\frac{1}{N}\sum(x_i-\mu)^3}{\left(\frac{1}{N}\sum(x_i-\mu)^2\right)^{3/2}}$
Min value X_{min}	$\min(x_i)$	*Kurtosis* -	$\frac{\frac{1}{N}\sum(x_i-\mu)^4}{\left(\frac{1}{N}\sum(x_i-\mu)^2\right)^2}$
Peak-to-peak $X_{P\text{-}P}$	$X_{max} - X_{min}$	*Waveform factor* -	$\frac{X_{rms}}{\frac{1}{N}\sum_{i=1}^{N}\lvert x_i\rvert}$
Mean(Average) μ	$\frac{1}{N}\sum_{i=1}^{N}x_i$	*Peak factor* -	$\frac{X_{max}}{X_{min}}$
RMS X_{rms}	$\sqrt{\frac{1}{N}\sum_{i=1}^{N}x_i^2}$	*Pulse factor* -	$\frac{X_{max}}{\frac{1}{N}\sum_{i=1}^{N}\lvert x_i\rvert}$
Variance σ^2	$\frac{1}{N}\sum_{i=1}^{N}(x_i-\mu)^2$	*Mean square value* -	$\frac{1}{N}\sum x_i^2$
Std. deviation σ	$\sqrt{\frac{1}{N}\sum_{i=1}^{N}(x_i-\mu)^2}$	*Clearance factor* -	$\frac{X_{max}}{(\frac{1}{N}\sum_{i=1}^{N}\sqrt{\lvert x_i\rvert})^2}$

Table 1. Time-domain features extracted from each denoised IMF. These features (seven dimensional and seven dimensionless) ensure that the characteristics of various soft fault types are captured.

4.2 Machine Learning Classifiers and Bayesian Optimization

The extracted feature vectors were used to train three different classifiers: Support Vector Machine (SVM), Extreme Learning Machine (ELM), and Extreme Gradient Boosting (XGBoost) are three distinct algorithms. SVM (10) creates a decision boundary with the maximum margin, making it suitable for small-to medium-sized datasets. Its primary hyperparameters include the regularisation parameter and kernel parameters, such as the width of the RBF kernel. The ELM (11) is a feedforward neural network with a single hidden layer, where the input weights are randomly set, and only the output weights are determined analytically; the number of hidden neurones is its main hyperparameter. XGBoost (12) constructs an ensemble of decision trees using gradient boosting, delivering top-tier performance; its hyperparameters encompass tree depth, learning rate, subsampling ratio, and regularisation terms.

To optimise performance, we applied Bayesian hyperparameter optimisation to each classifier. Bayesian optimisation constructs a probabilistic surrogate model, often a Gaussian process, to represent the objective function, which, in this case, is the classification accuracy. It employs an acquisition function, known as Expected Improvement, to effectively navigate the hyperparameter space. This method significantly reduces the number of evaluations required compared with a comprehensive grid search. In our setup, we tuned each model as follows: for SVM (RBF kernel), we tuned and ; for ELM, we tuned the number of hidden nodes; and for XGBoost, we tuned the tree depth, learning rate, and regularisation. We allocated approximately 50 Bayesian optimisation evaluations per model. The result is a more efficient search that consistently finds near-optimal parameters, thereby boosting classification accuracy without excessive computation.

Figure 2 illustrates the overall diagnostic workflow, which integrates ICEEMDAN decomposition, wavelet denoising, feature extraction, and Bayesian-optimised classification.

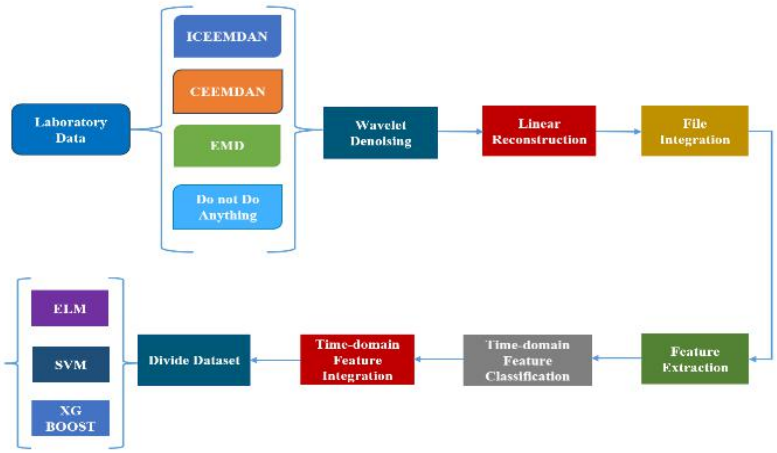

Figure 2. Flowchart of the DC–DC converter soft fault diagnosis process

5. EXPERIMENTAL SETUP

5.1 Fault and Circuit Design

The experimental validation was conducted on a 150 W DC–DC boost converter (input 10–32 V, output 12–35 V) using a UC3843 PWM controller and 100 Ω load. Table 2 lists the key specifications of the converter. The circuit includes two electrolytic capacitors and (nominal 1000 μF each). We focused on capacitor degradation because the aging of electrolytics is a common source of gradual faults in converters. We defined 16 operating conditions (fault modes) as follows.

- **f11:** Healthy baseline (both C_1 and C_5 within ±10% of nominal).
- **f12–f14:** Incremental degradation of C_1 by 10–50% (in 10% steps), with C_5 nominal.
- **f21–f24:** Incremental degradation of C_5 by 10–50%, with C_1 nominal.
- **f31–f44:** Simultaneous degradations of both C_1 and C_5 by 30–50% (combinations of 30–40% and 40–50% as detailed below).

These represent single- and dual-capacitor soft-fault scenarios. Table 3 specifies the exact capacitances and degradation ranges for each mode. For each scenario, high-resolution voltage and current measurements were collected under steady-state load conditions to produce a labelled multivariate time-series dataset. Figures 3–5 (circuit schematic, experimental platform, and physical converter) illustrate this setup.

Table 2. Specifications of the 150 W DC–DC Boost Converter.

Parameter	Specification
Circuit	150 W DC–DC boost converter
Input voltage	10–32 V
Output voltage	12–35 V
Input current	10 A (max)
Output current	6 A (max)

Table 3. Capacitive Degradation Modes in the 150 W Boost Converter (Fault Modes).

Fault Mode	C_1 (μF)	C_5 (μF)	Degradation Range (% for C_1/C_5)	Level
f11	988	916	0–10 / 0–10	1
f12	988	887	0–10 / 10–20	2
f13	988	653	0–10 / 30–40	3
f14	988	554	0–10 / 40–50	4
f21	864	916	10–20 / 0–10	5
f22	864	887	10–20 / 10–20	6
f23	864	653	10–20 / 30–40	7
f24	864	554	10–20 / 40–50	8
f31	655	916	30–40 / 0–10	9
f32	655	887	30–40 / 10–20	10
f33	655	653	30–40 / 30–40	11
f34	655	554	30–40 / 40–50	12
f41	546	916	40–50 / 0–10	13
f42	546	887	40–50 / 10–20	14
f43	546	653	40–50 / 30–40	15
f44	546	554	40–50 / 40–50	16

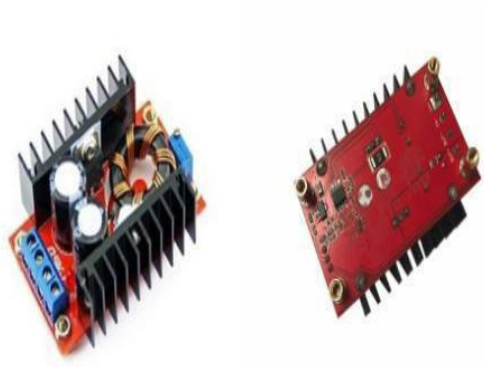

Figure. 3. Real Circuit Schematic of the 150w DC-DC boost converter

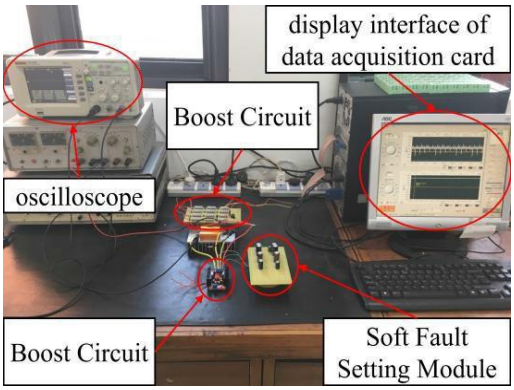

Figure. 4. Experiment Platform for the 150w DC-DC boost converter

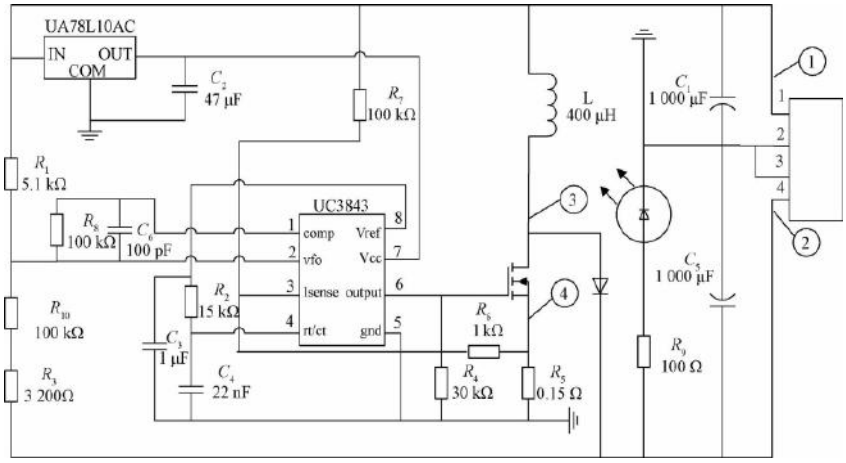

Figure.5. Boost converter Dc-Dc 150w

5.2 Data Collection and Training Protocols

We used a standard, supervised learning protocol. The data from all fault modes were randomly split into 70% training and 30% testing sets, which were stratified by class. This split was repeated 3–4 times using different random seeds to account for sampling variability. For each split, we trained the classifiers on the training set and evaluated them on the held-out test set. The performance metrics (accuracy and macro F1-score) were averaged (with standard deviation) across the trials.

In preprocessing, each test signal was decomposed by ICEEMDAN into approximately 4–6 IMFs until the residual became monotonic. Each IMF was then denoised via wavelet thresholding (a Daubechies wavelet with a universal threshold was used). Time-domain features (mean, RMS, variance, skewness, and kurtosis) were extracted from each denoised IMF, as described above. These IMF features were concatenated into a feature vector of approximately 20–30 dimensions for each sample.

For classification, we used an RBF-kernel SVM (tuning and), an ELM (tuning the number of hidden neurones), and an XGBoost model (tuning the tree depth, learning rate, and regularisation). Bayesian optimisation (Gaussian process surrogate, expected improvement) was applied with a budget of approximately 50 evaluations per model to determine near-optimal hyperparameters.

6. RESULTS AND DISCUSSION

6.1 Feature Extraction Comparison

The results confirmed that using ICEEMDAN for feature extraction yielded superior performance. In our experiments, ICEEMDAN consistently produced cleaner IMFs and more discriminative features than the basic EMD or CEEMDAN. For example, Table 4 shows that with XGBoost (no tuning), ICEEMDAN-based features achieve an average accuracy of 95.6 ±1.0%, whereas EMD-based features yield only 88.9 ±2.0%. The confusion matrices (omitted for brevity) indicate that mode mixing in plain EMD caused many misclassifications, whereas ICEEMDAN's adaptive decomposition greatly reduced such errors. The CEEMDAN-based features exhibited intermediate performance (untuned XGBoost: ~93.1% accuracy). Overall, ICEEMDAN produced the cleanest modes and most discriminative features. Applying wavelet denoising to these IMFs further improved the accuracy by removing the residual high-frequency noise.

Figure 6. Decomposition of a sample signal by (a) EMD, (b) CEEMDAN, and (c) ICEEMDAN.

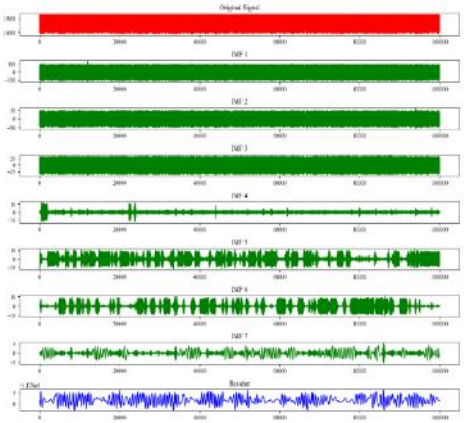

Figure 6. (1) IMFs Decomposition EMD

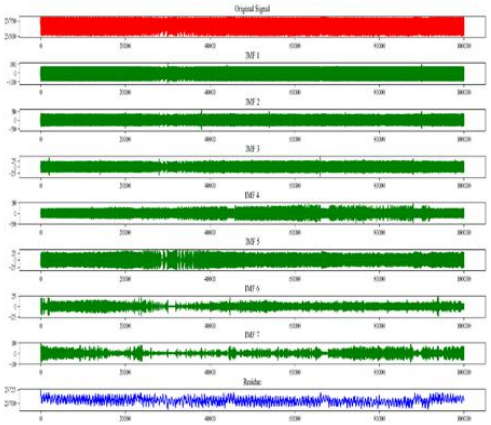

Figure 6. (2) IMFs Decomposition CEEMDAN

Figure 6. (3) IMFs Decomposition ICEEMDAN

6.2 Classifier Evaluation

Figure 7 (omitted) illustrates the confusion matrix for the best model (ICEEMDAN + XGBoost with Bayesian optimisation). The matrix was nearly diagonal, indicating that almost all the test samples were correctly classified. Only a few off-diagonal confusions occurred between adjacent fault levels (e.g. a slight misclassification between f23 and f24), which is expected given the gradual nature of the soft faults. Importantly, faults involving different components (e.g. f13 vs. f21) were never confused. The high values on the diagonal (often >90% for each class) indicate that the model reliably distinguishes between all fault conditions. For instance, with SVM+BO on a 70/30 split, the healthy class (f11) had a true-positive rate of approximately 97%, with only a few percent misclassified as the mildest fault (f12). In summary, the confusion matrices confirm that the proposed ICEEMDAN-based features enable accurate multiclass diagnosis, with residual errors occurring only between the most similar fault classes.

Figure 7. Confusion matrices for (a) XGBoost, (b) SVM, (c) ELM, and (d) Combined classifier (ICEEMDAN features).

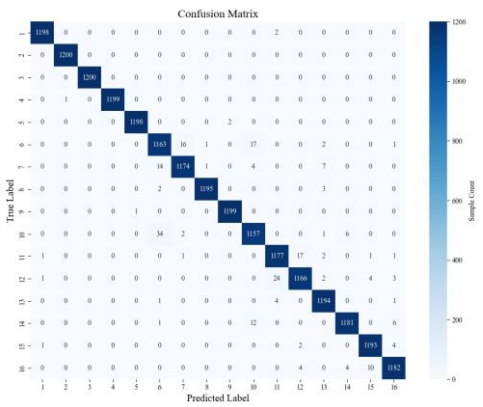

Figure 7. (a) XGBoost

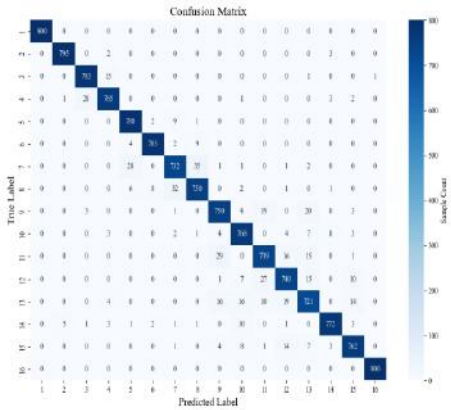

Figure 7. (b) SVM

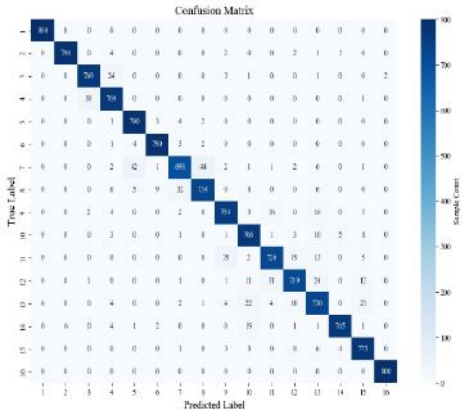

Figure 7. (c) ELM

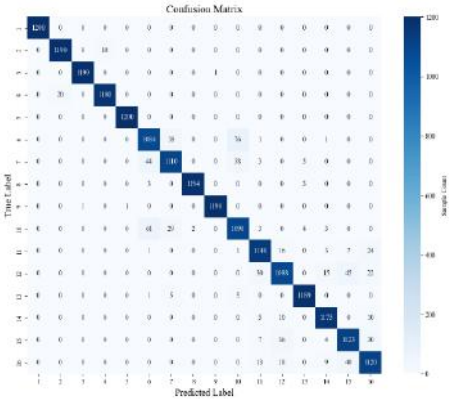

Figure 7. (d) Combined classifier

Across all classifiers (SVM, ELM, and XGBoost), Bayesian hyperparameter tuning consistently improved the performance by approximately 2–3%. XGBoost achieved the highest accuracy overall, reflecting its strong scalability. The combined pipeline (ICEEMDAN → wavelet denoising → feature extraction → BO-tuned classifier) significantly outperformed the alternatives based on plain EMD or CEEMDAN.

Tables 4 and 5 summarise the average classification accuracy and F1-scores (mean ± std) for all models for the 70/30 split. ICEEMDAN-based features yielded the highest scores in all cases. For example, ICEEMDAN+XGBoost achieved 95.6%±1.0% accuracy without tuning, which increased to 97.2%±0.6% with Bayesian optimisation (Table 4). In contrast, CEEMDAN+XGBoost achieved 93.1%±1.2% (no tuning) and 95.0%±1.0% (BO), while EMD+XGBoost gave 88.9%±2.0% and 91.5%±1.7%. The macro F1-scores in Table 5 show the same trend. These results confirm the effectiveness of our proposed approach.

Table 4. Classification accuracy (%) (mean ± std) for different decompositions and classifiers (70/30 split).

Decomposition	SVM	SVM (BO)	ELM	ELM (BO)	XGBoost	XGBoost (BO)
EMD	85.3 ± 2.1	88.7 ± 1.8	82.1 ± 3.5	86.2 ± 2.4	88.9 ± 2.0	91.5 ± 1.7
CEEMDAN	90.2 ± 1.9	93.4 ± 1.5	88.7 ± 2.3	91.9 ± 1.8	93.1 ± 1.2	95.0 ± 1.0
ICEEMDAN	94.5 ± 1.3	96.7 ± 0.8	92.0 ± 1.6	94.8 ± 1.2	95.6 ± 1.0	97.2 ± 0.6

Table 5. Macro F1-score (%) (mean ± std) for each model (70/30 split).

Decomposition	SVM	SVM (BO)	ELM	ELM (BO)	XGBoost	XGBoost (BO)
EMD	84.7 ± 2.2	87.9 ± 1.9	81.5 ± 3.4	85.4 ± 2.6	88.0 ± 2.1	90.8 ± 1.5
CEEMDAN	89.5 ± 2.0	92.7 ± 1.6	87.8 ± 2.5	90.8 ± 1.9	92.5 ± 1.3	94.3 ± 1.1
ICEEMDAN	93.8 ± 1.4	96.1 ± 1.0	91.5 ± 1.7	94.3 ± 1.3	94.8 ± 0.9	96.5 ± 0.7

6.3 Comparison with EMD and CEEMDAN

Traditional EMD suffers from severe mode mixing and often produces spurious components that obscure the fault features. For instance, when using XGBoost on EMD-derived features, the accuracy is limited (~89–92%), and confusion matrices show several misclassifications among similar fault classes. In contrast, ICEEMDAN's adaptive noise injection produced much cleaner modes, pushing the accuracy above 97% (with tuning). CEEMDAN (7) reduces the residual noise compared to EMD, but it still does not completely separate certain fault components. This resulted in a 3–5% accuracy drop relative to ICEEMDAN. In practice, classifiers using CEEMDAN features misclassify approximately 4–6% of samples, whereas ICEEMDAN limits errors to less than 3%, even for adjacent fault classes. Thus, ICEEMDAN provides a clear advantage in terms of soft-fault feature quality.

6.4 Noise Sensitivity Testing

We also evaluated the robustness to noise by adding white Gaussian noise to the test signals at different signal-to-noise ratios (SNRs): 20, 10, 5, and 0 dB. Classifiers trained on clean data were tested using these noisy signals. As expected, the accuracies of all models decreased as the SNR decreased. For the ICEEMDAN+XGBoost+BO model, the accuracy decreased from approximately 98% at 20 dB to 78% at 0 dB (see Table 6). The SVM and ELM models showed similar declines, although XGBoost consistently retained higher accuracy under noise. The relative drop in performance reflects the reduced distinguishability of fault features at a low SNR. These results indicate that ICEEMDAN coupled with wavelet denoising provides some noise immunity, but an extremely low SNR (e.g. 0 dB) significantly impairs feature extraction.

Table 6. Accuracy (%) of the ICEEMDAN+XGBoost+BO model under various SNR levels.

SNR (dB)	20	10	5	0
Accuracy	98%	92%	85%	78%

Figure 8. Accuracy of each model versus different SNR levels (XGBoost, SVM, and ELM).

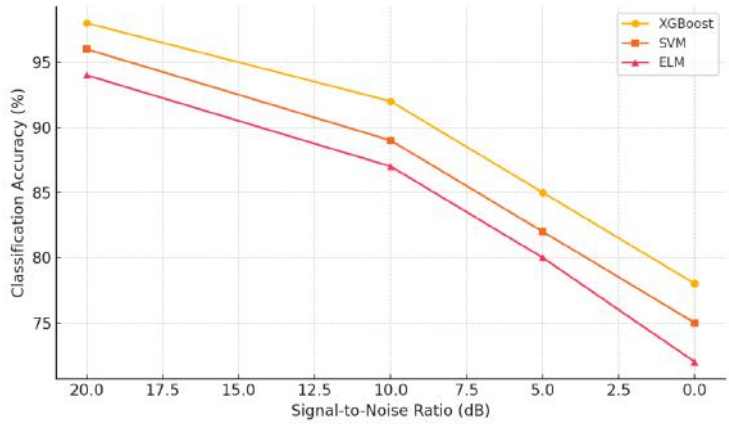

Figure 8. Model Accuracy vs. SNR Levels

7. CONCLUSION

This study introduces an innovative framework for detecting subtle soft faults in DC–DC converters. By combining ICEEMDAN signal decomposition, wavelet-based noise reduction, and Bayesian-optimised machine learning classifiers, this approach overcomes the limitations of conventional fault detection methods. Our results show that the ICEEMDAN-derived features significantly enhance the diagnostic accuracy compared to EMD and CEEMDAN. In particular, an XGBoost classifier tuned with Bayesian optimisation achieved an accuracy of up to 97.2% for multiclass fault identification. The integrated use of advanced signal separation, denoising, and hyperparameter tuning produces a robust fault detection system that maintains high precision, even under challenging conditions. This makes the method well-suited for critical applications (e.g. aerospace, power transmission, and renewable energy), where undetected soft faults can lead to costly failures.

Future work may focus on deploying this fault detection framework in real-time monitoring systems and exploring deep learning models to further improve accuracy. Extending this approach to other types of power electronic converters could broaden its applicability and reinforce its utility in various industrial and commercial settings.

REFERENCES

1. Mohan N., Undeland T. M., Robbins W. P., (2003): *Power Electronics: Converters, Applications, and Design* (3rd ed.). Wiley, Hoboken, NJ, USA.

2. Kazerani M., (2020): A review of DC-DC converter topologies for renewable energy systems. *IEEE Transactions on Power Electronics*, 35(2), 984–1002.
3. Blaabjerg F., Yang Y., Yang D., Wang X., (2018): Power electronics for renewable energy systems—Status and trends. *IEEE Transactions on Industrial Applications*, 54(6), 5814–5823.
4. Patel M. R., Naikan V. N. A., (2018): Fault diagnosis of DC-DC converters using signal processing and machine learning. *IEEE Transactions on Industrial Electronics*, 65(7), 5726–5736.
5. Cheng L., Qiu Z., Sripad K., (2019): A survey on fault diagnosis of power electronic circuits. *IEEE Access*, 7, 120985–121003.
6. Huang N. E. et al., (1998): The empirical mode decomposition and the Hilbert spectrum for nonlinear and non-stationary time series analysis. *Proceedings of the Royal Society A*, 454(1971), 903–995.
7. Torres M. E. et al., (2011): A complete ensemble empirical mode decomposition with adaptive noise. *IEEE Transactions on Signal Processing*, 60(5), 1056–1069.
8. Colominas M. A., Schlotthauer G., Torres M. E., (2014): Improved complete ensemble EMD: A suitable tool for biomedical signal processing. *Biomedical Signal Processing and Control*, 14, 19–29.
9. Donoho D. L., (1995): De-noising by soft-thresholding. *IEEE Transactions on Information Theory*, 41(3), 613–627.
10. Yan R., Gao R. X., (2007): Wavelet packets and their applications in machine fault diagnosis. *Mechanical Systems and Signal Processing*, 21(2), 793–805.
11. Randall R. B., (2021): *Vibration-Based Condition Monitoring: Industrial, Aerospace, and Automotive Applications*. Wiley, Hoboken, NJ, USA.
12. Lei Y. et al., (2020): Applications of machine learning to machine fault diagnosis: A review and roadmap. *Mechanical Systems and Signal Processing*, 138, 106587.
13. Cortes C., Vapnik V., (1995): Support-vector networks. *Machine Learning*, 20(3), 273–297.
14. Huang G. B., Zhu Q. Y., Siew C. K., (2006): Extreme learning machine: Theory and applications. *Neurocomputing*, 70(1–3), 489–501.
15. T. Chen and C. Guestrin, “XGBoost: A scalable tree boosting system,” in *Proc. 22nd ACM SIGKDD Int. Conf. Knowl. Discov. Data Min.*, 2016, pp. 785–794.